Egyptian Journal of Chemistry

http://ejchem.journals.ekb.eg/

CrossMark

Integrated 3D-QSAR and Docking Study of Alkylpiperazine-Based GSK-3β Inhibitors

Ismail Lamrani[1]*, Fathallaah Bazi [1], Fatiha Amegrissi[1], Bahija Mounir [1]*

[1]*Laboratory of Analytical and Molecular Chemistry, Faculty of Sciences Ben M'Sik, Hassan II University of Casablanca, Casablanca, Morocco*

Abstract

Glycogen synthase kinase-3β (GSK-3β), a protein kinase with diverse roles in various biological processes, has emerged as a promising target for drug research in the treatment of numerous clinical diseases. In this study, we employed a combination of computational techniques, including molecular docking and three-dimensional quantitative structure-activity relationship (3D-QSAR), to investigate a set of 36 alkylpiperazine derivatives as potential GSK-3β inhibitors. Our best-performing 3D-QSAR model yielded impressive conventional determination coefficients R^2 of 0.95 and leave-one-out cross-validation Q^2 of 0.56, showcasing its robustness and predictive capability. External validation using a test set of six compounds further confirmed the model's reliability, with anticipated R^2_{test} values of 0.87. To reinforce the validity of our 3D-QSAR model, a Y-Randomization test was conducted. Additionally, to investigate the binding interactions between the most active chemical and the GSK-3β protein's active site (Protein Data Base ID: **1Q4L**, we used molecular docking simulations. These docking results not only corroborated the findings from our 3D-QSAR analysis but also provided valuable insights into the binding mode of alkylpiperazine derivatives with GSK-3β. These results are very interesting, and they help us understand how alkylpiperazine compounds interact with GSK-3β. This information is important for creating new and strong GSK-3β inhibitors. These inhibitors could be used to treat different diseases.

Keywords: Alkylpiperazine derivatives; CoMFA; GSK-3β; Molecular docking; 3D-QSAR

INTRODUCTION

The glycogen synthase kinase 3β was initially discovered and investigated for its roles in the control of glycogen synthase, the rate-limiting enzyme in glycogen production [1]. It is a serine/threonine kinase with two isoforms found in mammals (α and β). These isoforms exhibit widespread cellular expression, significant levels of homology (>90%) at the catalytic domain, and similar biochemical characteristics [2]. The fact that GSK-3β has a variety of natural substrates, including ATP, and that most ligands work by competing with ATP contributes to the fact that GSK-3β is essential for glucose homeostasis and CNS function [3]. This requires the development of approaches that address non-selectivity in the design of potential GSK-3 inhibitor therapeutic candidates. Similar computational drug design studies targeting Ribonucleic Acid RNA-binding proteins such as RNA Binding Fox-1 Homolog 1 (RBFOX1) have successfully demonstrated the utility of in silico methods for discovering potent anti-cancer compounds [4]. This reinforces the relevance of employing 3D-QSAR and docking in the development of selective GSK-3β inhibitors

There is still a need to create more strong and selective small compounds that demonstrate an inhibitory activity towards this desirable receptor due to the limitation of GSK-3 selective inhibitors [5-9]. For this reason, a series of some potent GSK-3β inhibitors: Alkylpiperazine derivatives have been developed and published by (Kohara et all) [10] However, many recent research have shed some light on kinases inhibitors [11], [12]; therefore, Knowing this kind of moieties and how they bind can help researchers find effective anti-cancer drugs. Our intention is to create novel compounds with increased GSK-3β inhibitory activity by means of an in-silico investigation based on this series. Medicinal researchers most commonly use two techniques for drug design and discovery: ligand-based and structure-based. Based-ligand approach includes the well-known 3-QSAR models, Comparative Molecular Field Analysis (CoMFA) [13] which is based on changes in 3D structural features of molecules such as steric, electrostatic properties. The structure-based technique, which incorporates molecular docking, evaluates the interactions of a ligand within the protein's active site. In order to anticipate the activity of the newly designed

_____

leads prior to their synthesis, a QSAR model must be created. Because a successful QSAR model helps to understand relationships between the structural features and biological activity of any class of molecules, and provides researchers a deep analysis about the lead molecules to be used in further studies [14].
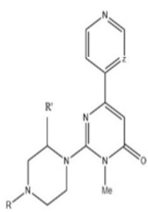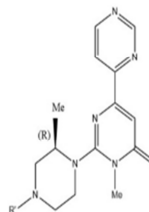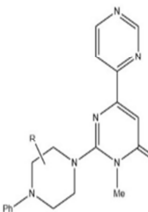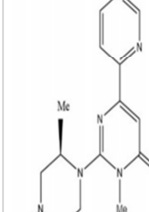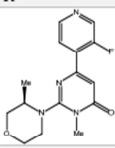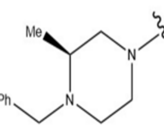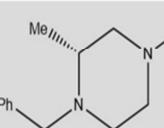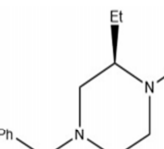
In the present study, 3D-QSAR (CoMFA) study following by docking molecular simulation were performed on a series of thirty-six alkylpiperazine derivatives [10] to determine the essential structural features needed to create new potent lead candidates for this class. The results extracted from this study might be helpful to design highly potent GSK-3β inhibitors.

2. MATERIAL AND METHODS

2.1. Data set for 3-QSAR and Molecular Docking Studies

The 36 compounds that were studied were all taken from earlier research that was published. Table 1 displays the IC_{50} (nM) values that were converted to $-log10$ (pIC_{50}) values for the current study. [10] The dataset was divided into two sets: The test set was utilized to evaluate the performance of the proposed model, and the training set, which consisted of thirty randomly selected molecules used to create the quantitative model.

Table 1: The GSK-3β inhibitory actions and chemical structures of substituted alkylpiperazine derivatives (* Test set).

No	R	R'	No	R'	No	Piperazine	No	Ar
1	(structure)		11	i-Pr	19	(structure)	22	2-F-Ph
2	C-H	Me	12	PhCH2			23	3-F-Ph
3	C-H	Me	13*	Ph			24	4-F-Ph
4	N	Me	14	MeCO			25	4-Cl-Ph
5	N	Me	15	PhCO			26	2-MeO-Ph
6	C-H	Me	16*	MeOCO	20	(structure)	27*	3-MeO-Ph
7	C-H	Me	17	MeSO2			28*	4-MeO-Ph
8*	N	Me	18	4-MePhSO2			29	2-CN-Ph
9	N	Me					30	3-CN-Ph
10	N	H					31	4-CN-Ph
							32	4-Py
					21	(structure)	33*	3-Py
							34	2-Py
							35	2-pyrimidinyl
							36	5-pyrimidinyl

2.2. Molecular Modeling

The molecular modeling tool SYBYL-X 2.0 (Tripos Inc., St. Louis, USA) was utilized for molecular modeling and docking experiments (3D & Docking) on a 64-bit Windows 10 workstation. Chemsketch version 12.0 (ACD lab) was used to sketch the structures of every chemical. Subsequently, they were minimized employing the Powell method with a convergence criterion of 0.01 kcal/mol Å, utilizing the Tripos standard force field [15] and Gasteiger-Hückel atomic partial charges [16]. All structures are cleaned, and 3D optimized.

_____

2.3. Computational Methods
2.3.1. Molecular Alignment

Molecular alignment is essential for the progression of any 3D-QSAR (Three-Dimensional Quantitative Structure-Activity Relationship) study [17][18]. Figure 1 illustrates the suggested alignment process, where all the molecules were aligned using the distil alignment technique provided by SYBYL. This alignment was performed with respect to the most potent inhibitor, which was selected as a reference molecule for fitting the remaining compounds in both the training and test sets of alkylpiperazine derivatives. Compound 29 was specifically chosen as the reference for aligning the dataset in 3D-QSAR investigations and for creating template molecules to generate contour maps.
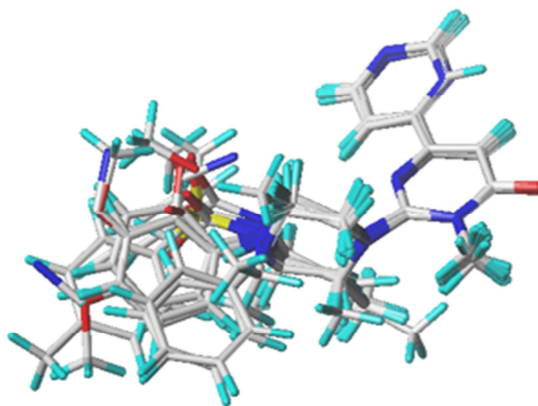

Figure 1: Training set alignment and 3D-QSAR structure superposition using molecule 29 as a template

2.3.2. CoMFA Studies

CoMFA was used to analyze the steric and electrostatic energies of the Tripos force fields in SYBYL-X 2.0 [19]. The probe was an sp^3 carbon atom with a charge of +1.0 and a van der Waals radius of 1.52 Å. It was inserted at each lattice point of the lattice box to determine the electrostatic (Coulomb potential) and steric (Lennard-Jones potential). Analyses were conducted on a 3D grid with 2.0 Å spacing in all Cartesian directions. The standard cut-off energy for both steric and electrostatic fields was set at 30 kcal/mol [20].

2.3.3. Partial Least Square (PLS) Analysis

The PLS regression approach [21] is commonly employed to evaluate the linear correlation between independent variables (CoMFA) and the target variable (GSK-3β inhibitory activity (pIC_{50})) due to the multitude of variables resulting from field calculations. Initially, cross-validation (Q^2) is performed using the leave-one-out (LOO) method [22], where one compound is removed from the training set and its inhibitory activity is predicted by the model using the remaining compounds. This process is repeated until each compound has been excluded once. The model with the highest Q^2 value, lowest standard error of prediction (Scv), and fewest components is selected. To diminish noise and expedite the analysis, the column filtering threshold (σ) is set at 2.0 kcal/mol. Subsequently, after determining the optimal number of components, they are employed to construct the final PLS model without a validation method [23], [24], aiming to achieve the highest determination coefficient (R^2).

2.3.4. Validation and Predictive Power of the Model

The primary objective of each QSAR study is to identify a model with optimal predictive and generalization abilities. Consequently, a test set comprising six chemicals was utilized to evaluate the predictive performance of the developed 3D-QSAR models. These molecules were aligned using the previously described methods, and the resultant CoMFA model from the training set was applied to predict their activities.

2.3.5. Y-Randomization Test

The models we derived underwent additional validation using the Y-Randomization method [25]. The activities of studied molecules (pIC_{50}) are randomly shuffled multiple times and a new QSAR model is generated after each iteration. Compared to the original models, we predict that the Q^2 and R^2 values of these new QSAR models will be lower. This method attempts to eliminate the potential for random correlations. If, in the Y-Randomization process, we obtain higher Q^2 and R^2 values, it indicates that it is not feasible to generate a reliable 3D-QSAR model for this dataset due to structural redundancies and the possibility of chance correlations.

2.4. Molecular Docking

A molecular docking investigation was conducted utilizing Autodock Vina and Autodock. tools1.5.4, to interpret the obtained results from CoMFA contour map.

A grid box (x = 24, y = 24, z = 24 at 1 Angstrom spacing) was created to include the binding site in **1Q4L**, and the bioactive conformations were simulated with Autodock Vina [27]. The docking protocol's ligand and protein preparation phases were

_____

accomplished using Autodock tools 1.5.4 from the MGL Tools package [26]. The programs PyMol [29] and Discovery studio 2016 [28] were used to analyze the data.

2.4.1. Macromolecule Preparation

The crystal structure of GSK-3β was obtained from the Protein Data Bank, http://www.rcsb.org/ (PDB entry code: **1Q4L**). None of the ligands under investigation were found to be bound to the protein in the Protein Data Bank (PDB). As a result, the original ligand associated with the protein was removed. Subsequently, we performed docking experiments with both the most active and least active ligands from our dataset into the active site of the target receptor. To prepare the PDB file for these docking studies, we used Discovery Studio 2016, This included taking out of the protein model every ligand, cofactor, and solvent molecule.

2.4.2. Ligand Preparation

The ligands chosen for docking were modeled in a manner consistent with the approach used in the 3D-QSAR studies. Three-dimensional structures of these ligands were constructed using the Chemsketch tool within SYBYL. Subsequently, these structures underwent minimization employing the Tripos standard force field [16] and were assigned Gasteiger-Hückel atomic partial charges [17]. The minimization was carried out using the Powell method with a convergence threshold set at 0.01 Kcal/mol Å.

3. RESULTS AND DISCUSSION

Table 2 presents the residual values of the corresponding predicted and experimental activity values for the training and test sets of the CoMFA model.

Table 2: Observed and predicted inhibitory activity (pIC50) of compounds in both the training and test sets for the final CoMFA model (* Test set).

N°	pIC$_{50}$ (obs)	pIC$_{50}$ (pred)	
		CoMFA	**Residu**
1	8.155	8.165	-0.010
2	7.538	7.687	-0.149
3	7.079	7.403	-0.324
4	7.886	7.867	0.019
5	7.658	7.409	0.249
6	6.036	6.585	-0.549
7	6.000	6.502	-0.502
8*	7.119	6.689	0.430
9	6.000	6.526	-0.526
10	6.201	6.861	-0.660
11	7.886	7.680	0.206
12	8.081	8.635	-0.554
13*	8.854	8.634	0.220
14	7.310	7.497	-0.187
15	7.678	7.341	0.337
16*	7.155	6.874	0.281
17	7.337	7.212	0.125
18	7.721	7.501	0.220
19	6.108	6.080	0.028
20	6.000	5.932	0.068
21	7.367	7.587	-0.220
22	9.699	9.445	0.254
23	9.301	9.042	0.259
24	9.398	9.430	-0.032
25	8.921	8.929	-0.008
26	9.097	9.028	0.069
27*	9.699	9.107	0.592
28*	10.000	9.741	0.259
29	8.377	8.445	-0.068
30	8.658	8.892	-0.234
31	8.569	8.309	0.260
32	8.420	8.231	0.189
33*	8.409	8.114	0.295
34	8.387	8.506	-0.119
35	7.620	7.922	-0.302
36	7.854	7.848	0.006

_____

_____

3.1. CoMFA Results

A 3D-QSAR model has been developed to elucidate and quantitatively predict the impact of substituents' steric and electrostatic fields on the inhibitory activity of thirty alkylpiperazine derivatives, utilizing CoMFA descriptors available in SYBYL.

As discussed earlier, CoMFA model was generated for the alignment method shows in Figure 1, distil rigid alignment method gave the best statistical results; therefore, it is used in the present study. Table 2 displays the statistical parameters obtained for the CoMFA model, including Q^2, R^2, R^2_{test}, F-t, and Scv, as determined by SYBYL. A Q^2 value exceeding 0.5 is considered significant, indicating a correlation with a confidence level exceeding 95%. For our chosen CoMFA model, the cross-validated determination coefficient Q^2 for the training set is 0.56, and the non-crossvalidated determination coefficient R^2 is 0.95. We utilized five principal components, which is a reasonable choice given the number of molecules used to construct the model. The standard error was found to be 0.1. Furthermore, to validate the model's predictive capacity, we conducted external validation, resulting in an R^2_{test} value of 0.87. These statistical findings underscore the robust stability and excellent predictive performance of the developed CoMFA model.

3.2. Contour analysis

Figures 2a and 2b illustrate the contour maps for the final CoMFA model. In the steric map, green contours (representing an 80% contribution) designate regions where the presence of bulky substituents enhances the activity. Conversely, yellow contours (with a 20% contribution) indicate regions where bulky groups diminish the activity.

In the electrostatic map, blue contours (also with an 80% contribution) indicate areas where electronegative substitutions enhance the activity. Conversely, red contours (with a 20% contribution) denote regions where electropositive substitutions increase the activity. Since Compound 29 is the most active within the series, it was selected as the reference structure for generating these contour maps. Specifically, with Compound 29: a) In the steric fields, the green contour around the phenyl group signifies that bulky groups are advantageous. Consequently, based on the CoMFA electrostatic contours, electron-donor groups such as a methoxy group can enhance the activity, while the presence of a phenyl group tends to decrease the activity.
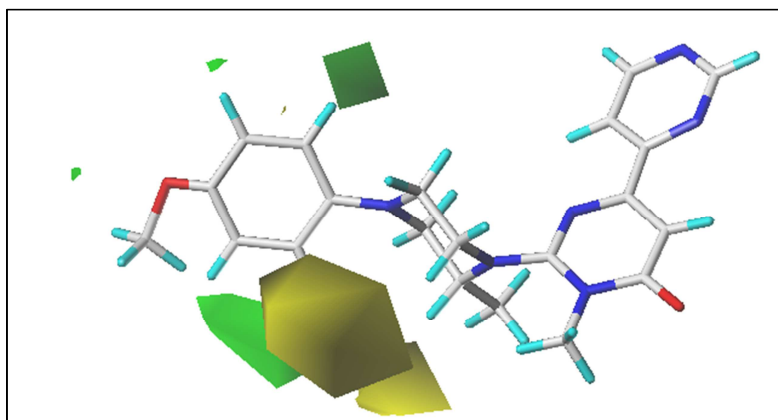

Figure 2a: Std* coeff. CoMFA assessment contour maps with a 2 Å grid spacing when combined with compound 29. Steric fields: Regions with higher activity levels are indicated by green outlines (80% contribution), whereas regions with lower activity levels are indicated by yellow contours (20% contribution).
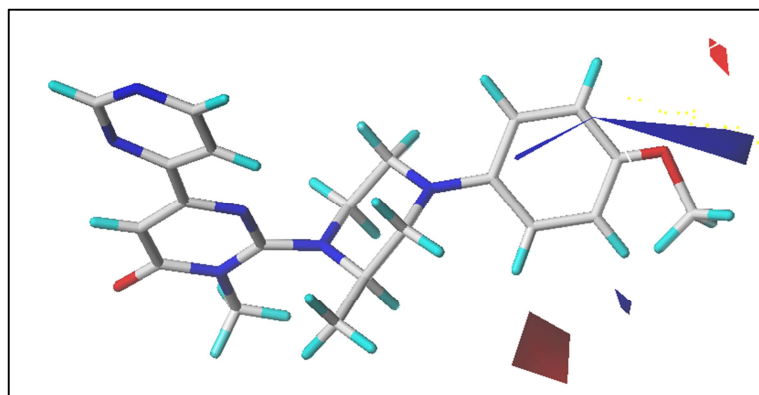

Figure 2b: Std* coeff. CoMFA assessment contour maps with a 2 Å grid spacing when combined with compound 29. Electrostatic fields: Regions with negative charges are indicated by blue outlines (80% contribution) while those with positive charges are indicated by red contours (20% contribution).

_____

_____

3.3. External validation

The most important part of every QSAR study is model validation. Thus, a true and reliable model should be able to predict a precise activity in the external test set [26].

The activity of the final six molecules was therefore predicted using the CoMFA model that was derived from a training set of thirty alkylpiperazine derivatives; Table 3 displays the parameters pertaining to the models' performance.

Table 3: Presents statistics for the CoMFA Model using partial least squares (PLS).

Model	Q^2	R^2	S_{cv}	F-t	N	R^2_{test}	Fractions	
							Ster	Elec
CoMFA	0.56	0.95	0.112	64.36	5	0.87	0.604	0.396

Q2: Cross-validated determination coefficient
N: Optimal number of components obtained from cross-validated PLS analysis,
R²: Non-cross-validated correlation coefficient.
Scv: squared coefficient of variation
.F-t: F-test value.
R²test: External validation determination coefficient.

3.4. Y-Randomization

The CoMFA model was subjected to validation using the Y-Randomization method. This involved multiple random shuffling iterations of the dependent variable, followed by the creation of a 3D-QSAR model. The outcomes of this analysis are presented in Table 4. The favorable results observed in our original CoMFA model cannot be attributed to a fortuitous correlation within the training set. This conclusion is supported by the consistently low Q^2 and R^2 values obtained after each shuffling iteration, confirming the robustness of our findings.

Table 4: Q^2 and R^2 values after several Y-Randomization tests

Iteration	CoMFA	
	Q^2	R^2
1	0.23	0.65
2	-0.11	0.83
3	-0.089	0.86
4	-0.267	0.77
5	-0.118	0.57
6	-0.292	0.68

3.5. Docking Molecular results

Molecular docking was used to analyze how GSK-3β inhibitors attach and the residues implicated in the interaction. The binding pocket of GSk-3β kinase is mostly supplied by residues GLU 268, ASP 264, LYS183, ASP 260, GLN 185, ASP 264, and LYS 183. The binding mechanism of compound 29 is shown in Figure 3.

Docking of the highly active molecule 29 revealed the formation of a hydrogen bond with the active site residue GLU 268. Because compound 29 is a covalent inhibitor, its Mickael electrophilic site is close to GLU 268, allowing for a covalent. This explains the elevated activity of compound 29, as determined by CoMFA contour map analysis.

The concept of dual-target pharmacology has gained traction for diseases requiring high specificity, such as tuberculosis [30]. This strategy echoes our aim in targeting GSK-3β selectively, where molecular docking of compound 29 revealed precise binding interactions, reinforcing its therapeutic promise through mechanism-specific inhibition.

Future work could benefit from integrating synthetic approaches such as microwave-assisted methodologies to rapidly generate analogs with optimized pharmacophores, like the strategies employed in the synthesis of imidazolone derivatives with proven antimicrobial properties [31].
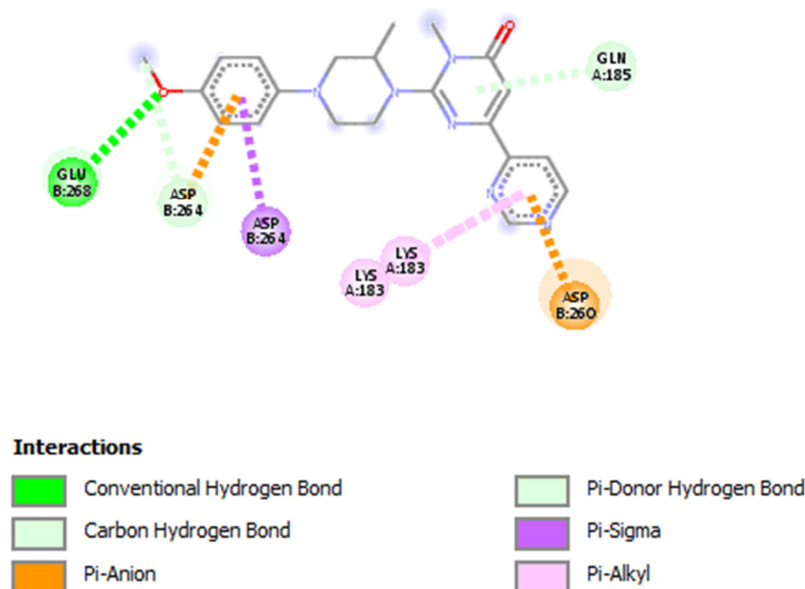
_____

_____

Figure 3: The docked conformation derived for the most active chemical 29 appears in two dimensions.

4. CONCLUSION

This work used a combined computational method to understand how several GSK-3β inhibitors inhibit their target. When a 3D-QSAR investigation was first carried out, the model was shown to be statistically significant. Using leave-one-out, Y-Randomization, and an external test set, the robustness of the model was demonstrated, and the final CoMFA showed predictiveness. Also, the docking of compound 29, which is the most active, into the suggested binding site of GSK-3β was examined. Docking results indicates the most active compound shows the interactions such as hydrogen bonds and the distance of the Michael electrophilic group of the inhibitor to the GLU 268 residu with receptor which explain the stability of ligand inside receptor. The combination of these molecular modeling results will provide the information required for better understanding of structural features necessary for inhibitory activity of alkylpiperazine derivatives analogs.

Disclosure statement: Conflict of Interest: All authors certify that they have no affiliations with or involvement in any organization or entity with any financial interest or non-financial interest in the subject matter or materials discussed in this manuscript.

Compliance with Ethical Standards: This article does not contain any studies involving human or animal subjects.

References
[1] Lan S., Catherine P., Bruce R.C., Lori W., Jun Z.X., Richard A.L., Mary B., Jerry R., William V.M., Demarest K.T., Gee-Hong K. (2004), *Bioorg. Med. Chem.*, 12, 1239-1255.
[2] Davies G., Jiang W.G., Mason M.D. (2001) The interaction between beta-catenin, GSK3beta and APC after motogen induced cell–cell dissociation, and their involvement in signal transduction pathways in prostate cancer, *Int. J. Oncol.*, 18, 843–847. DOI: 10.3892/ijo.18.4.843
[3] Conrad K., Kathrin L., Maryse L., Laurent M., Thomas L. (2004), *Bioorg. Med. Chem. Lett.*, 14, 413-416. DOI: 10.1016/j.bmcl.2003.10.062
[4] Ul Qamar M.T., P. Sanz-Jimenez, S.R. Banoon, X. Tong Zhu, F.M. Aldakheel, N.M. Almansour, L.A. Aldaji, W.A.I. Al-Megrin, F. Ahmed, Computational identification of anti-cancer compounds targeting the RNA-binding domain of human FOX-1 protein (RBFOX1), *Resul. Chem.*, (2024), 13, 102204. DOI: 10.1016/j.rechem.2024.102004
[5] Yoganathan T.N., Costello P., Chen X., Jabali M., Yan J., Leung D., Zhang Z., Yee A., Dedhar S., Sanghera J. (2000) Integrin-linked kinase (ILK): a ``hot'' therapeutic target, *Biochem. Pharmacol.*, 60, 1115–1119. DOI: 10.1136/ard.2007.079822
[6] Wang M., Li X., Meintzer M.K., Laessig T., Birnbaum M.J., Heidenreich K.A. (2000) Cyclic AMP promotes neuronal survival by phosphorylation of glycogen synthase kinase 3beta, *Mol. Cell Biol.*, 20, 9356–9363. DOI: 10.1074/jbc.M109.067785
[7] Xavier I.J., Mercier P.A., McLoughlin C.M., Ali A., Woodgett J.R., Ovsenek N. (2000), Glycogen synthase kinase 3☐ negatively regulates both DNA-binding and transcriptional activities of heat shock factor 1, *J. Biol. Chem.*, 275, 29147–29152. DOI: 10.1002/j.1460-2075.1990.tb07419.x

_____

[8] Ali A., Hoeflich K.P., Woodgett J.R. (2001) Glycogen synthasekinase-3: properties, functions, and regulation, *Chem. Rev.*, 101, 2527–2540. DOI: 10.1021/cr000110o

[9] Mandelkow E.M., Mandelkow E. (1998) Tau in Alzheimer's disease, *Trends Cell Biol.*, 1998, 8, 425–427. DOI: 10.1016/s0962-8924(98)01368-3

[10] Kohara T., Nakayama K., Watanabe K., Kusaka S., Sakai D., Tanaka H., Fukunaga K., Sunada S., Nabeno M., Saito K., Eguchi J., Mori A., Tanaka S., Bessho T., Takiguchi-Hayashi K., Horikawa T. (2017) Discovery of novel 2-(4-aryl-2-methylpiperazin-1-yl)-pyrimidin-4-onesas glycogen synthase kinase-3β inhibitors, *Bioorganic & Medicinal Chemistry Letters* 27, 3733–3738. DOI: 10.1016/j.bmcl.2013.09.021

[11] Qingxiu H., Chu H., Guangping L., Haiqiong G., Yuxuan W., Yong H., Zhihua L., Yuanqiang W. (2020) In silico design novel (5-imidazol-2-yl-4-phenylpyrimidin-2-yl)[2-(2-pyridylamino)ethyl]amine derivatives as inhibitors for glycogen synthase kinase 3 based on 3D-QSAR, molecular docking and molecular dynamics simulation, *Computational Biology and Chemistry* 88, 107328. DOI: 10.1016/j.compbiolchem.2020.107328

[12] Akhtar M., Bharatam P.V. (2012) 3D-QSAR and Molecular Docking Studies on3-Anilino-4-Arylmaleimide Derivatives as Glycogen Synthase Kinase-3β Inhibitors, *Chem. Biol. Drug Des.*, 79, 560–571. DOI: 10.1111/j.1747-0285.2011.01291.x

[13] Kubinyi H. (2003) Comparative Molecular Field Analysis (CoMFA), *Handb. Chemoinform.*, 1555-1574. DOI: 10.1002/9783527618279.ch44d

[14] Gupta S.P., Mathur A.N., Nagappa A.N., Kumar D., Kumaran S. (2003) A quantitative structure-activity relationship study on a novel class ofcalcium-entryblockers:1-[(4-(Aminoalkoxy)phenyl) sulphonyl]indolizines, *Eur. J. Med. Chem.*, 38(10), 867-873. DOI: 10.1016/j.ejmech.2003.08.001

[15] Clark M., Cramer R.D., Opdenbosch N.V. (1989) Validation of the general purpose tripos 5.2 force field, *J. Comput. Chem.*, 10(8), 982-1012. DOI: 10.1002/jcc.540100804

[16] Purcell W.P., Singer J.A. (1967) A brief review and table of semi empirical parameters used in the Hueckel molecular orbital method, *J. Chem. Eng. Data*, 12, 235-246. DOI: 10.1021/je60033a020

[17] AbdulHameed M.D.M., Hamza A., Liu J., Zhan C.G. (2008) Combined 3D-QSAR modeling and molecular docking study on indolinone derivatives as inhibitors of 3-phosphoinositide-dependent protein kinase-1, *J. Chem. Inf. Model.*, 48(9), 1760-1772. DOI: 10.1021/ci800147v

[18] El-Mernissi, R. El khatabi K, Khaldan A, ElMchichi L, Ajana M. A, Lakhlifi T, and Bouachrine M. "3D- QSAR, ADMET, and Molecular Docking Studies for Designing New 1,3,5-Triazine Derivatives as Anticancer Agents." *Egypt. J. Chem* 65, no. 132 (2022): 9–18. DOI.org/10.21608/ejchem.2022.76000.3715.

[19] Cramer R.D., Patterson D.E., Bunce J.D. (1988) Comparative Molecular Field Analysis (CoMFA), 1. effect of shape on binding of steroids to carrier proteins, *J. Am. Chem. Soc.,* 110(18), 5959-5967. DOI: 10.1021/ja00226a005

[20] Ståhle L., Wold S. (1988) Multivariate data analysis and experimental design in biomedical research, *Prog. Med. Chem.*, 25, 291-338. DOI: 10.1016/s0079-6468(08)70281-9

[21] Wold S. (1991) Validation of QSAR's, *Quant. Struct. Relationships* 10(3), 191-193. DOI: 10.1002/qsar.19910100302

[22] Cruciani G., Baroni M., Clementi S., Costantino G., Riganelli D., Skagerberg B. (1992) Predictive ability of regression models. Part i: standard deviation of prediction errors (SDEP), *J. Chemom.*, 6(6), 335-346. DOI:10.1002/cem.1180060604

[23] Baroni M., Clementi S., Cruciani G., Costantino G., Riganelli D., Oberrauch E. (1992) Predictive ability of regression models. Part ii: selection of the best predictive PLS model, *J. Chemom.*, 6, 347-356. DOI:10.1002/cem.1180060605

[24] Golbraikh A., Tropsha A. (2002) Beware of Q2!, *J. Mol. Graph. Model.*, 20(4), 269-276. DOI: 10.1016/s1093-3263(01)00123-1

[25] Rücker C., Rücker G., Meringer M. (2007) Y-randomization and its variants in QSPR/QSAR, *J. Chem. Inf. Model.*, 47(6), 2345-2357. DOI: 10.1021/ci700157b

[26] Morris G.M., Goodsell D.S., Halliday R.S., Huey R., Hart W.E., Belew R.K., Olson A.J. (1998) Automated docking using a lamarckia genetic algorithm and and empirical binding free energy function, *J. Comput. Chem.*, 19, 1639-1662. DOI: 10.1002/jcc.21256

[27] Trott O., Olson A.J. (2010) AutoDock vina: Improving the speed and accuracy of docking with a new scoring function, efficient optimization, and multithreading, *J. Comput. Chem.*, 31(2), 455-461. DOI: 10.1002/jcc.21334

[28] Dassault Systèmes BIOVIA, Discovery Studio Modeling Environment, Release 2017, San Diego: Dassault Systèmes. Available from: *http://accelrys.com/products/collaborative-science/biovia-discovery-studio/*

[29] DeLano W. (2017) The PyMOL Molecular Graphics System DeLano Scientific, Palo Alto, CA, USA. Available from: *http://www.pymol.;org*

[30] A.N. Hussein, M. Fawzi, R.F. Obaid, S.R. Banoon, E.S. Abood, A. Ghasemian, Dual pharmacological targeting of Mycobacterium tuberculosis (Mtb) PKNA/PKNB: A novel approach for the selective treatment of TB illness, *Egypt. J. Chem.*, (2022), 65(12), 409-419. DOI: 10.21608/EJCHEM.2022.135419.5981

[31] Z.R. Banoon, R.S. Mahmood, A.R. Hamad, Z.A. Hussein, Design, microwave synthesis, characterization and antimicrobial activity of imidazolone derivatives, *J. Mol. Struc.*, (2025), 1322, 140701. DOI: 10.1016/j.molstruc.2024.140701

_____

Egypt. J. Chem. **68,** SI: Z. M. Nofal (2025)